A New Color Space for Color Skin Detection Using Quadratic Programming

Ali Khayati[1*], Saeed Mirghasemi[2]

[1] Department of Computer & IT Engineering, Parand Branch, Islamic Azad University, Tehran, Iran.
[2] School of Engineering and Computer Science, Victoria University of Wellington, Wellington, New Zealand.

[*] Corresponding author. Email: khaiiaty@gmail.com
Manuscript submitted July 10, 2017; accepted September 8, 2017.
doi: 10.17706/ijcee.2018.10.1.31-45

Abstract: A new skin-based color space is introduced in this paper that can be effectively used for skin detection. Converting to the new space is performed through a linear matrix multiplication. The mission is to address how to obtain the weights of the conversion matrix so that the new space can discriminate skin regions. Quadratic programming is used to obtain the weights of the conversion matrix by optimizing the distances between the color components of some sample skin and non-skin pixels. The new Quadratic Programming-based Color space (QPC) uses a new form of distance metric under some specific criteria. Otsu's thresholding method as a post-processing technique is applied to the converted image in QPC to binarize the image for detection purposes. Common skin image benchmarks is used to evaluate the performance of the proposed method. Experiments shows that the proposed method hands in a conversion matrix that can be used effectively to discriminate skin in a wide range of images, and produces better results in comparison to some standard color spaces and classification algorithms.

Key words: New color space, skin detection, quadratic programming, Otsu's thresholding, connected component analysis.

1. Introduction

1.1. Color Spaces

The usage of color in image processing is motivated by two principal factors. First, color is a powerful descriptor that often simplifies object identification and extraction from a scene. Second, human can discern thousands of color shades and intensities, compared to about only two dozen shades of gray [1]. The purpose of a color space (also called color model or color system) is to facilitate the specification of colors in some standard generally-accepted way [1]. A color model is an abstract mathematical model describing the way colors can be represented as tuples of numbers, typically as three or four values or color components (e.g. RGB and CMYK are color models). Many color spaces are related to each other by linear transformations that are captured by 3×3 matrices. Hence a given color, and thereby any color image, can be represented in terms of another color space by transforming its 3D vector representation using a 3×3 matrix. For instance, the calculation performed in the color space conversion from RGB to YIQ is presented below:

$$\begin{bmatrix} Y \\ I \\ Q \end{bmatrix} = \begin{bmatrix} 0.299 & 0.587 & 0.114 \\ 0.596 & -0.275 & -0.321 \\ 0.212 & -0.523 & 0.311 \end{bmatrix} \begin{bmatrix} R \\ G \\ B \end{bmatrix} \quad (1)$$

The main advantage of segmentation through using color features is that object detection can be

performed independently of the size and position of the object within the image [2]. In most cases, the segmentation of a color image demonstrates to be more useful than the segmentation of a monochrome image, because the color image exhibits much more image features than the monochrome image [3]. The segmentation of a color image requires a computational cost, which is considerably higher than what is needed for the monochrome image, but it is no longer a major problem with the increasing speed of computation and decreasing cost of color sensors. In fact, there has been a remarkable growth of techniques for the segmentation of color images in the past decade. Among the populous number of papers which have used color features for object detection or color segmentation, we focus on reviewing those that have created a new color space for detection purposes. Several color spaces are developed for skin and face detection [4]-[6]. De Dios et al. in [5] have presented a new color space, YCgCr, using the smallest color difference (G-Y) instead of (B-Y) which is the biggest difference and is selected in YCbCr. A new color space and a level set method based on Mumford-Shah model for skin region segmentation is performed in [6]. Another new color space has been constructed for skin color clustering in [4], and the concept of correlation between the image data and the color of illuminants is introduced. Other applications also had excuses for creating new color spaces. For example, a new color space for bladder tumor detection is proposed in [7]. In this new color space, they applied a non-linear transformation to the fluorescence component which leads to a better separation of fluorescing and non-fluorescing pixels. Jia et al. [8] have presented a thresholding approach based on a new color space model and embedded it into the background subtraction. An approach to detect specular highlights in color images is presented in [9]. Panetta et al. [10] have introduced a method of splitting up color spaces into different components and then performing edge detection on individual color planes. A new color space was also introduced which is an improved version of the PCA algorithm. By analyzing the results of these algorithms, they determined which color space and edge detector is best suited for each algorithm. A similar work to what we are about to introduce has been introduced by us in [11], in which we have similarly used a 3×3 conversion matrix to create a target-based color space via linear and quadratic conversions. The Particle Swarm Optimization (PSO) algorithm is used to search for the optimum weights of the conversion matrix by optimizing the objective function of the FCM clustering method.

Next, to show the importance of color features from different color space, we briefly mention some of the very recent publications using color features and color spaces for detection tasks. A new morphological operations is introduced in [15] for color image boundary detection using the CIELab color space in spherical coordinates. Another approach proposed in [14], uses the CIELab color space to reduce the interference of backgrounds for airport detection using visual saliency model and support vector machine. Using simple color features in the RGB color space, a fast fire detection algorithm is proposed in [13] using K-medoids clustering and particle swarm optimization. A preprocessing technique based on non-linear conversion model for the HSV color space is proposed in [12] to facilitate the geometric bleeding and tumor detection utilizing the new geometry image feature. RGB color space is combined with Lab color space in [16] to create feature vectors of each image patch for visual saliency detection that produces better saliency map compared to both primary color spaces.

1.2. Quadratic Programming

A linearly constrained optimization problem with a quadratic objective function is called a quadratic program (QP). Because of its many applications, quadratic programming is often viewed as a discipline in and of itself. The concept is ubiquitous in image processing. Particularly, For image classification, it has been widely used via Support Vector Machines [17]-[20]. Markov random fields (MRF)-based interactive image segmentation techniques, is another field in which the quadratic programming plays an important role [21]-[24]. In these methods, the user labels a small subset of pixels, and the MRF propagates these labels

across the image, typically by finding high-gradient contours as segmentation boundaries where the labeling changes.

A probabilistic segmentation method based on Markov Random Fields was presented in [21], in which the authors investigate the convex case of the Quadratic Markov Measure Fields with application in image segmentation. Fu *et al.* [22] present an alternative continuous relaxation approach to image labeling which makes use of a quadratic cost function over the class labels, and [23] obtained a multiplicative fixpoint that quickly solves very large quadratic programs on low-cost parallel compute devices, and demonstrated applications to super resolution and image segmentation. Also, quadratic programming has been used for image segmentation based on a new graph-theoretic formulation of clustering [25], object detection [26], [27] Abnormality Segmentation in Brain Images [28], and 3D image segmentation [29].

The main goal of the presented paper is to create a new skin-based color space in which some features of classes to be classified are introduced to the classifier through human interference. The features are simple color components of skin and non-skin pixels of sample images in the RGB space, and the classifier is a simple matrix conversion which has proper weights to fulfill our goal towards discrimination. Meanwhile, the main advantages of the proposed method to other conventional methods are:

a) It uses simple properties (i.e. color features) directly to get trained. This means no prior computation is needed to extract features.

b) The number of training data is too small compared to the number of total data to be classified.

c) The parameter acquisition for the classifier is simple (i.e. forming the quadratic formulas according to the color components of skin and non-skin and then solving it through the renowned quadratic programming theorem).

d) It benefits from a simple classification procedure which is a matrix multiplication.

e) Once the conversion matrix is obtained, the classification is fast to implement.

f) The conversion matrix is applicable to other images independently (i.e. no need to perform the training process)

The organization of the paper is as follows. In Section 2, formulations of the quadratic distances, the contemplated constraints, and the Otsu's method are presented. Next, in Section 3, the discrimination behaviors of the new color space, and the detection results of the new method in different skin databases are presented. To support our theory, the detection results are compared with other state-of-the-art or classic methods. Finally, Section 4 summarizes the conclusions and future lines of the research.

2. The Proposed Method

The block diagram of the new skin discrimination method is presented in Fig. 1. To create the Quadratic Programming-based Color space (QPC), we need a conversion matrix for some sample pixels from skin and non-skin regions in an image is needed. Therefore, very small sub-images of skin and non-skin are extracted manually from the original image in the RGB color space in form of 30×30 images. We call these sub-images training samples from now on. Next, these sample images are converted from the RGB color space to a new space using an unknown parametric 3×3 matrix according to Eq. (2):

$$\begin{bmatrix} X_1 \\ X_2 \\ X_3 \end{bmatrix} = \begin{bmatrix} w_{11} & w_{12} & w_{13} \\ w_{21} & w_{22} & w_{23} \\ w_{31} & w_{32} & w_{33} \end{bmatrix} \begin{bmatrix} R \\ G \\ B \end{bmatrix} \tag{2}$$

in which $X = [X_1\ X_2\ X_3]$ is the vector of the color components of each pixel in the new space, R,G, and B are color components of the pixel in the RGB color space, and w_{ij} ($i = 1,2,3$ and $j = 1,2,3$) are the to-be-obtained weights of the conversion matrix. The equation should be repeated for all the pixels in the training

samples.

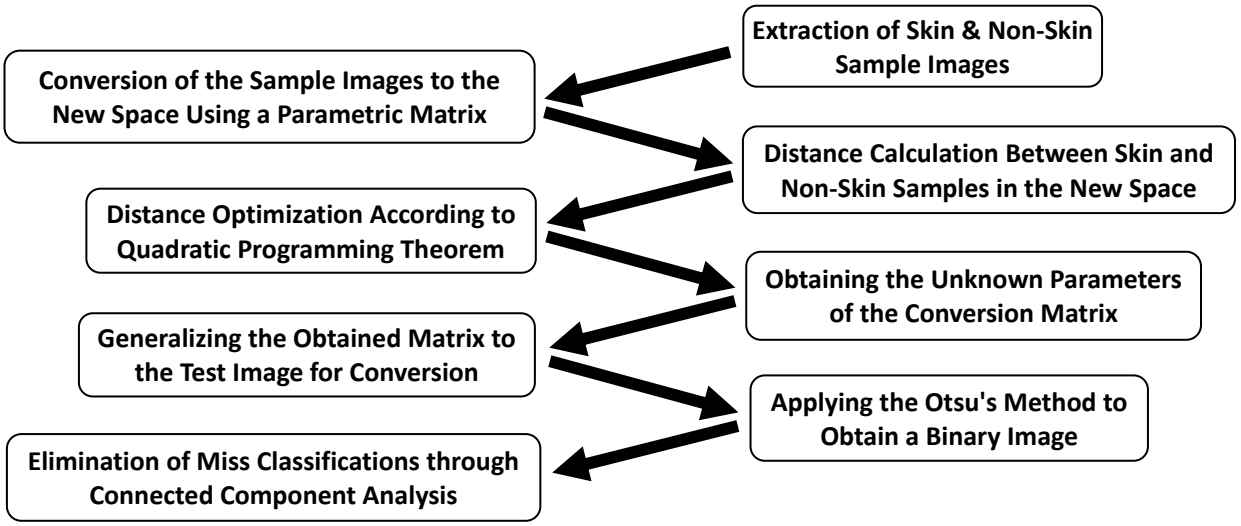

Fig. 1. Different steps of the new proposed skin detection method.

There are two significant objectives in obtaining the weights of the conversion matrix as depicted in Fig. 2. First, a maximum distance between the skin and non-skin cluster centers in the new color space, and second, a minimum entropy in the color components of each cluster's pixels. These criteria are established to achieve weights for the conversion matrix that lead to a better separation between skin and non-skin pixels. Therefore, as depicted in Fig. 2, after converting the training samples to the new space using Eq. (2), we form three types of distances according to the color components of the converted pixels:

i. Distances between converted skin pixels and their class center.
ii. Distances between converted non-skin pixels and their class center.
iii. Distance between the two class centers.

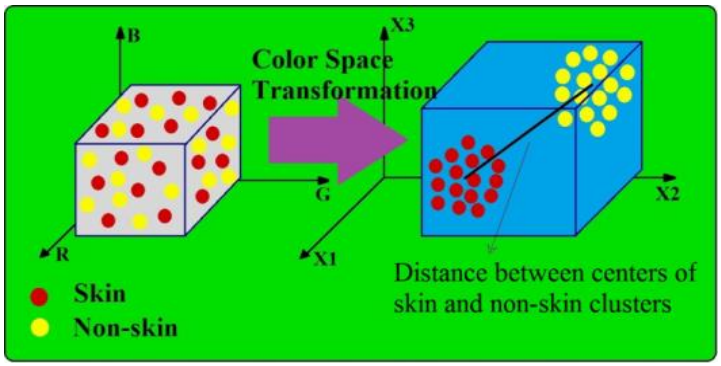

Fig. 2. The visual criteria for target and non-target pixels separation after conversion to the new color space.

Next, we minimize the first two distances, and maximize the third one according to quadratic programming optimization where the weights of the conversion matrix are variables with unknown values. The center of each class is simply the mean of each channel color value for all the pixels inside that class. When the values of the conversion matrix are calculated, it is used to convert the whole image to the new color space. In the next section, we will describe how to use Eq. (2) and color components of skin and non-skin pixels to derive the above mentioned distances in form of a quadratic function to be optimized through quadratic programming.

2.1. Cost Function; the Quadratic Distances

From Eq. (2), a unique pixel in the new color space can be represented by three components; X_1, X_2 and X_3 as follows:

$$\begin{aligned} X_1 &= w_{11}R + w_{12}G + w_{13}B \\ X_2 &= w_{21}R + w_{22}G + w_{23}B \\ X_3 &= w_{31}R + w_{32}G + w_{33}B \end{aligned} \tag{3}$$

As mentioned before, the distance calculation between color components of pixels after conversion should regard three important matters: the distance of each skin pixel from its class center, the distance of each non-skin pixel from its class center, and the distance between skin and non-skin class centers. We want the first two distances as minimum as possible, and the third one as maximum as possible. To be able to use quadratic programming for this optimization, the mentioned distances should be determined in a quadratic manner. Therefore, we establish a quadratic function, $\psi(W)$, and use it as an objective function in the quadratic programming as:

$$\psi(W) = \sum_{i=1}^{M+N} d_i^2 - L_i^2 \tag{5}$$

where $\psi(W)$ is a function of W, the conversion matrix. d_i denotes the distances of each skin and non-skin pixel from its class center (the above mentioned i and ii distances), L is the distance between the two class centers (the above mentioned iii distance), and M,N are the number of skin and non-skin pixels respectively. First, centers of the two clusters must be obtained:

$$\begin{aligned} \mu_{X1}^1 &= w_{11}\bar{R}^1 + w_{12}\bar{G}^1 + w_{13}\bar{B}^1 \\ \mu_{X2}^1 &= w_{21}\bar{R}^1 + w_{22}\bar{G}^1 + w_{23}\bar{B}^1 \\ \mu_{X3}^1 &= w_{31}\bar{R}^1 + w_{32}\bar{G}^1 + w_{33}\bar{B}^1 \end{aligned} \tag{5}$$

$$\begin{aligned} \mu_{X1}^2 &= w_{11}\bar{R}^2 + w_{12}\bar{G}^2 + w_{13}\bar{B}^2 \\ \mu_{X2}^2 &= w_{21}\bar{R}^2 + w_{22}\bar{G}^2 + w_{23}\bar{B}^2 \\ \mu_{X3}^2 &= w_{31}\bar{R}^2 + w_{32}\bar{G}^2 + w_{33}\bar{B}^2 \end{aligned} \tag{6}$$

where μ_{Xi}^1 and μ_{Xi}^2 are the cluster centers for the ith color component of skin and non-skin classes respectively, $\bar{R}^1, \bar{G}^1, \bar{B}^1$ are the mean values of skin pixels' component, and $\bar{R}^2, \bar{G}^2, \bar{B}^2$ are the mean values of non-skin pixels' component. From (4), (5), and (6), d_i and L are calculated as follows:

$$d_i^2 = \begin{cases} (\mu_{X1}^1 - X_{1i})^2 + (\mu_{X2}^1 - X_{2i})^2 + (\mu_{X3}^1 - X_{3i})^2 \\ (\mu_{X1}^2 - X_{1i})^2 + (\mu_{X2}^2 - X_{2i})^2 + (\mu_{X3}^2 - X_{3i})^2 \end{cases} \tag{7}$$

$$L^2 = (\mu_{X1}^1 - \mu_{X1}^2)^2 + (\mu_{X2}^1 - \mu_{X2}^2)^2 + (\mu_{X3}^1 - \mu_{X3}^2)^2 \tag{8}$$

Before optimizing the objective function, it is useful to review the Quadratic Programming theorem. Quadratic programming is a mathematical modeling technique designed to optimize the usage of limited resources. It has led to a number of interesting applications and the development of numerous useful results [30]-[36]. A quadratic programming problem is an optimization problem involving a quadratic

objective function and linear constraints. It can be stated in the general form of:

$$\text{Min} \quad Z = \sum_{j=1}^{n} c_j x_j + \frac{1}{2} \sum_{i=1}^{n} \sum_{j=1}^{n} q_{ij} x_i x_j \tag{9}$$

$$\text{s.t.} \quad \sum_{j=1}^{n} a_{ij} x_j \leq b_i, \quad i = 1, \dots, m, \tag{9-1}$$

$$x_j \geq 0, \quad j = 1, \dots, n. \tag{9-2}$$

In vector–matrix notation, it may be written as:

$$\begin{aligned} Min \quad & Z = cx + x^{\wedge\prime} Qx \\ s.t. \quad & Ax \leq b \\ & x \geq 0 \end{aligned} \tag{10}$$

where $x = (x_j, j = 1, \dots, n)$ is the vector of decision variables to be determined. The others are the parameters given by the problem: $c = (c_j, j = 1, \dots, n)$ is vector of cost coefficients, $Q = \|q_{ij}\|$ is the matrix of the quadratic form, $b = (b_i, i = 1, \dots, m)$ is vector of right-hand sides, and $A = \|a_{ij}\|$ is the matrix of constraint coefficients. In this paper, Q is symmetric and positive semi-definite. The problem is to determine the values of the decision variables under the constraints that minimize the objective function.

The method of Lagrange multipliers is a powerful tool for solving this category of problems without the need to explicitly solve the conditions, and use them to eliminate extra variables. In the Lagrange multiplier technique, a new variable λ is added to the problem, and the problem reduces to the minimization of a specific function as:

$$F(W, \lambda) = \psi(W) + \lambda C(W) \tag{11}$$

where $C(W)$ includes all the constraints of equalities and inequalities. To optimize, it is sufficient to solve the following equations:

$$\begin{cases} \frac{\partial F(W,\lambda)}{\partial W} = 0 \\ \frac{\partial F(W,\lambda)}{\partial \lambda} = 0 \end{cases} \tag{12}$$

2.2. Constraints

To ensure an effective conversion, it is obligatory to restrict matrix weights under several constraints. We have recognized four groups of them as follows:

1) In Eq. (3) for R, G and B equal to one, X_1, X_2 and X_3 are forced into one for each pixel in skin and non-skin clusters through the following constraints:

$$\sum_{j=1}^{3} w_{ij} = 1 \qquad for\ i = 1,2,3. \tag{13}$$

This equation tries to keep the mentioned point of RGB space in the same position in new color space, to prevent shrinkage of the space under the defined mapping. That is, the origin of RGB maps to the origin of

the new space.

2) Each RGB pixel In Eq. (3) regardless of its cluster is forced to take a new position in the RGB space. So, all pixels must be mapped under the 3D presentation rules. For a pixel in the new space, these rules include not having values more than the upper limit of a representable color space, as well as not having values less than its lower limit. In other words, we cannot depict pixels with color values more than 255 and less than zero if we want to stay loyal to image representation in the RGB space. These constraints could be committed with the assumption of the second and third groups of constraints as follows:

$$X_i \leq 255 \qquad for\ i = 1,2,3. \tag{14}$$

3) In Eq. (3), as discussed before, we should consider the lower side limitations as follows:

$$X_i \geq 0 \qquad for\ i = 1,2,3. \tag{15}$$

4) This constraint expresses a range of growth for all matrix weights. To have a homogenous transformation, all weights must be limited into a predefined range.

$$a \leq w_{ij} \leq b \tag{16}$$

According to a wide range of experiments using different images, we set $a = 6$ and $b = -6$.

It can be seen that $\psi(W)$ is a quadratic function of unknown weights. Now, this problem has changed to one of the most common problems in calculus, which is finding minima (in general, "extrema") of a function subject to a number of constraints. By solving the quadratic distances under the mentioned constraints, we obtain a 3×3 matrix which is used to convert the whole image into the new space. The idea is to generalize the conversion matrix obtained from the color properties of a limited number of pixels, for the whole image.

2.3. Image Segmentation using Otsu's Thresholding Method

Image binarization has been widely used in document image analysis, medical image processing, and scene analysis. Therefore, it is important in image segmentation and object detection to do a gray-level thresholding based on a proper threshold value to extract objects from their background. A variety of techniques have been proposed in this regard like [37] and [38] which utilize information concerning neighboring pixels (or edges) in the original picture to modify the histogram to make it useful for thresholding. Another class of methods deals directly with the gray-level histogram by parametric techniques. For example, the histogram is approximated in the least square sense by a sum of Gaussian distributions, and statistical decision procedures are applied [39]. However, such a method requires considerably tedious and sometimes unstable calculations [40]. Moreover, in many cases, the Gaussian distributions turn out to be a poor approximation of the real modes [40].

The Otsu's method [40] is a nonparametric and unsupervised method of automatic threshold selection, which maximizes the separability of the resultant classes using gray-level histogram, makes each cluster as tight as possible, and hopefully minimize their overlap. The algorithm assumes that the image to be thresholded contains two classes of pixels, or bi-modal histogram (e.g. foreground and background) then calculates the optimum threshold separating those two classes so that their combined spread (intra-class variance) is minimal. For these reasons, we have chosen the Otsu's method to apply to the image obtained in the QPC where we have different levels of intensity for skin and non-skin regions, in order to have a segmented black and white image. In Otsu's method we exhaustively search for the threshold that minimizes the intra-class variance, defined as a weighted sum of variances of the two classes:

$$\sigma_{\omega}^2(t) = \omega_1(t)\sigma_1^2(t) + \omega_2(t)\sigma_2^2(t) \quad (17)$$

Weights ω_i are the probabilities of the two classes separated by a threshold t and σ_i^2 variances of these classes. Otsu showed that minimizing the intra-class variance is the same as maximizing inter-class variance:

$$\sigma_b^2(t) = \sigma^2 - \sigma_{\omega}^2(t) = \omega_1(t)\omega_2(t)[\mu_1(t) - \mu_2(t)]^2 \quad (18)$$

which is expressed in terms of class probabilities ω_i and class means μ_i. The class probability $\omega_1(t)$ is computed from the histogram as t:

$$\omega_1(t) = \sum_{0}^{t} p(i) \quad (19)$$

while the class mean, $\mu_1(t)$ is:

$$\mu_1(t) = \sum_{0}^{t} p(i) * x(i) \quad (20)$$

where $x(i)$ is the value at the center of the ith histogram bin. Similarly, one can compute $\omega_2(t)$ and $\mu(t)$ on the right-hand side of the histogram for bins greater than t. The class probabilities and class means can be computed iteratively. This idea leads to an effective algorithm described below:

1) Compute histogram and probabilities of each intensity level.
2) Set up initial $\omega_i(0)$ and $\mu_i(0)$.
3) Step through all possible thresholds $t = 1, \ldots, maximum\ intensity$ to:
4) Update ω_i and μ_i
5) Compute $\sigma_b^2(t)$
6) The desired threshold corresponds to the maximum $\sigma_b^2(t)$.

2.4. Small Connected Component Elimination

It is very probable in skin images that the skin regions form connected areas that create large parts in the image. Depending on the size of the image, eliminating small connected components, can remove a large number of small false positives, as depicted in the next section. We have used the 8-connectivity component presented in [41], for connected component labeling and then small connected component elimination.

3. Experimental Results and Discussion

The proposed method is evaluated from different viewpoints in skin discrimination domain. The test images are gathered from famous and standard face/skin databases, plus various images suitable for this mean. First, we compare the new color space with some classic color spaces in Fig. 3. The figure illustrates the degree of separability of skin from its background in RGB, YCbCr, HSV, YIQ and QPC color spaces.

To visualize the discrimination between color components of skin and non-skin in the QPC more intuitively, the 3D plot of the color components of some random pixels from both skin and non-skin regions for the image in Fig. 3-e are shown in Fig. 4 before and after conversion. Each pixel has been placed in a cube according to its triple color components. This figure clearly shows that the two previously mentioned criteria are reasonably satisfied. First, the two regions have less entropy, and second, they have more distance between them.

It is possible to apply a conversion matrix to a wide range of images even without performing the training process. For example, by performing the previous optimization process, with the extracted training samples

shown in Fig. 5-b,c from the image in Fig. 5-a, the following matrix is obtained:

$$w = \begin{bmatrix} 0.1792 & 0.0222 & -0.0014 \\ 1.2000 & 0.2000 & -1.2000 \\ 1.2000 & 0.2000 & -1.2000 \end{bmatrix} \quad (21)$$

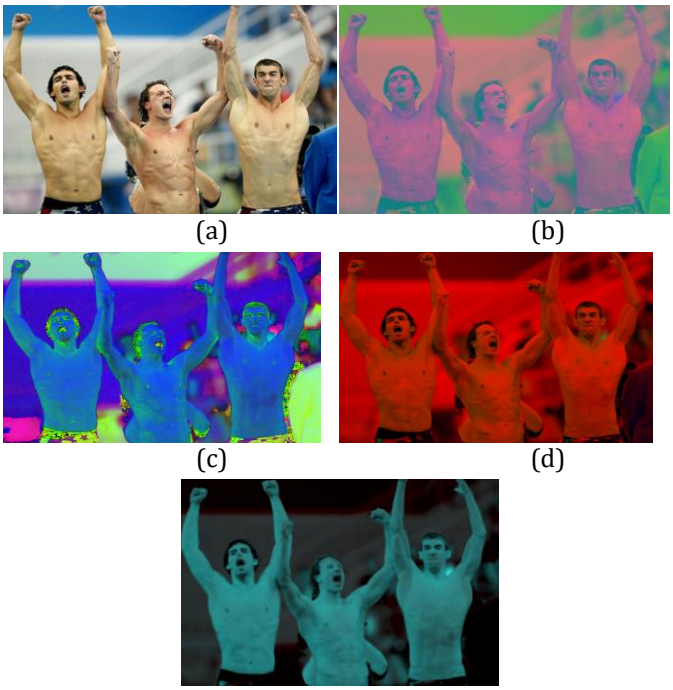

(a) (b) (c) (d) (e)

Fig. 3. Comparing a test image in several classic color spaces with the QPC. a) The original image. The conversion of (a) into the: b) YCbCr color space. c) HSV color space. d) YIQ color space. e) QPC.

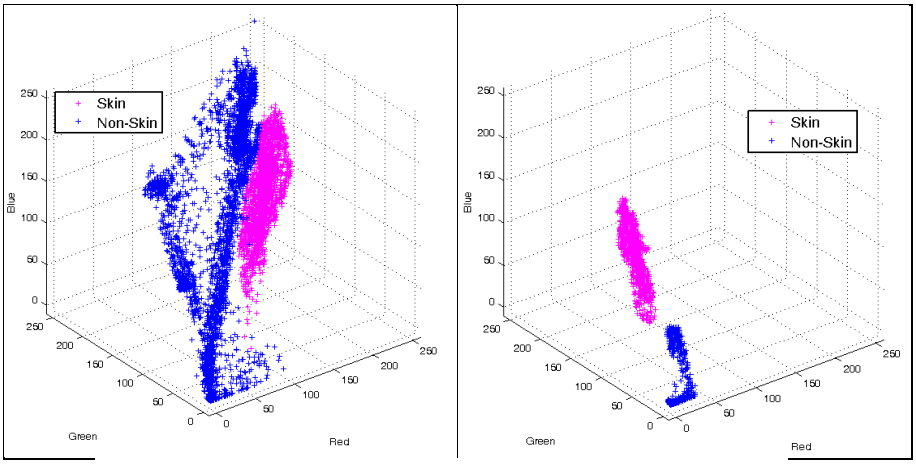

(a) (b)

Fig. 4. The 3D plot of skin and non-skin pixels distribution from Fig. 3-e before and after conversion. a) Distribution in the RGB color space. b) Distribution in the QPC.

The image in Fig. 5-a is intentionally selected for the optimization process because the non-skin regions in it include a large spectrum of colors, even those that have color components close to that of skin. Since, the skin color has a specific color range and continuity in value, the above matrix could be effectively applied to other images regardless of the database, lighting conditions and complexity of the image. Fig. 6 shows the capability of skin detection in several images in which all the images have been converted with

the same matrix in Eq. (21). The images have been chosen with various lighting and complexity properties to evaluate the discrimination abilities of the obtained matrix from different perspectives.

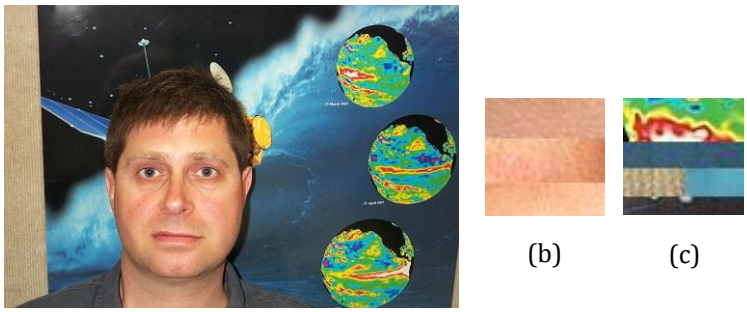

(a) (b) (c)

Fig. 5. A sample image used to obtain a versatile conversion matrix. a) The original image. b) Skin sample. c) Non-skin sample.

Fig. 6 shows that the converted images to the QPC contain bright and dark regions related to skin and non-skin respectively. However, the two mentioned categories are composed of pixels with different intensities. As explained in section 2.3, to obtain a black and white image in which they correspond to non-skin and skin part of an image respectively, the Otsu's thresholding method is applied to the images in the QPC. Fig. 7 shows several images in their original form (the RGB color space), in the QPC, after applying Otsu's method, and after eliminating small false positives regions. Performing the proposed method leads to effective results even in images with complex background.

Fig. 6. Converted results for different pictures while using a similar conversion matrix.

Thus far, the skin detection process is reduced to three simple steps; the first one is to multiply all pixels

of an image with the matrix in Eq. (21), the second one is applying the Otsu's thresholding method which is also applicable in a few seconds, and if necessary an small region elimination is performed. Table 1 provides the time needed for skin detection in images of different sizes. The type of hardware configuration may change these measures. The PC we have used has an Intel(R) core(TM) i7 CPU (2630QM @2.00 GHz) with 8 GB of RAM. The measured time is up to the end of the Otsu's method.

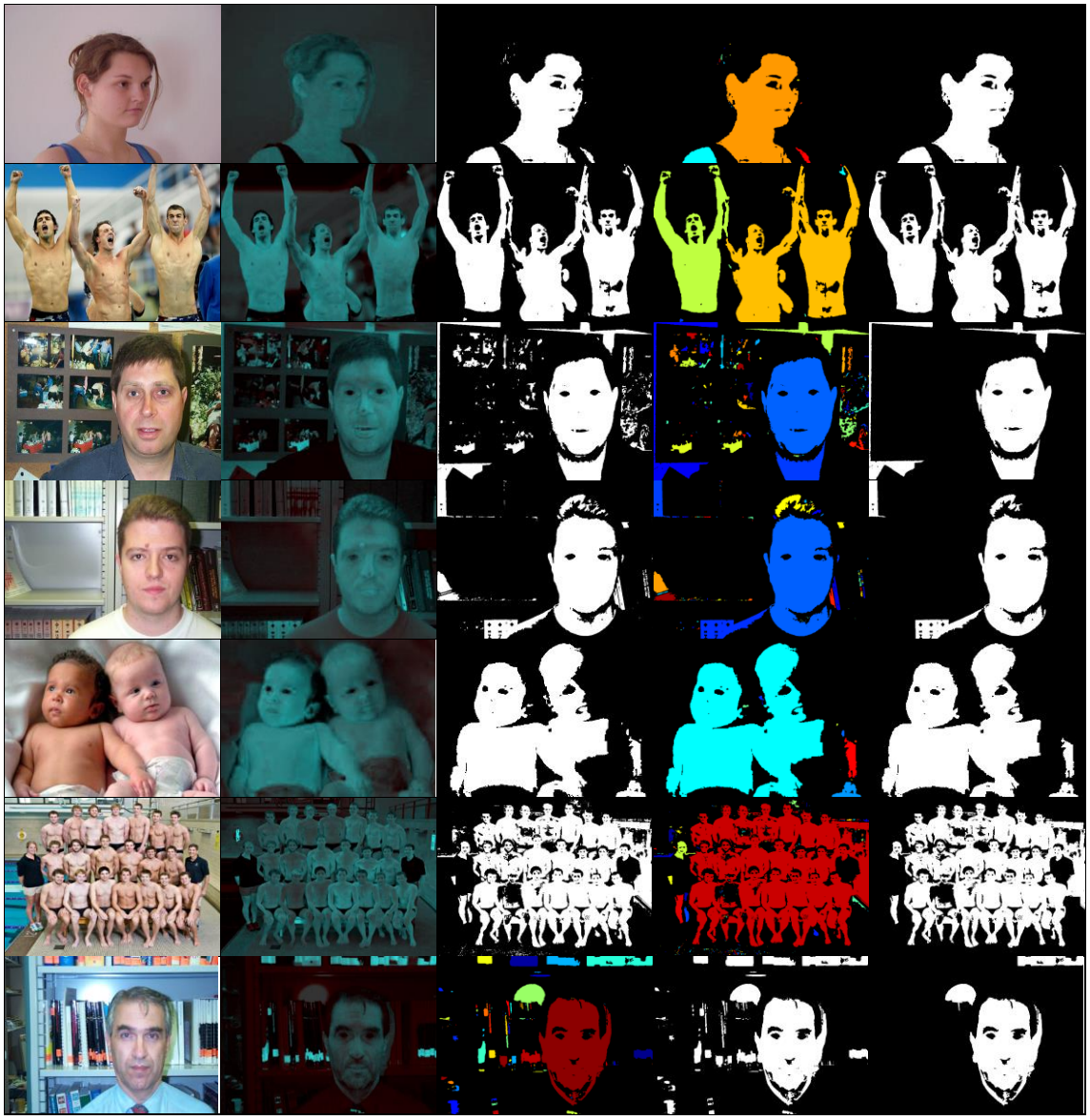

(a) (b) (c) (d) (e)

Fig. 7. Skin detection results in different images, including images with complicated background. a) The original image. b) Image in QPC. c) Otsu's thresholding results. d) Labeling different regions. e) Eliminating small regions.

Final detection results of the new method are even comparable with the results from non-linear classifiers, i.e. classifiers in which the classification procedure is done through a non-linear optimization or conversion procedure like what kernel methods do. In Fig. 8, the proposed method is compared with one of the most renowned classifiers, the Support Vector Machine (SVM). In this test, the kernel function of SVM is the Gaussian Radial Basis (rbf) with a default scaling factor, sigma, of 1. Column (b) in Fig. 8 shows the skin detection results of our method before omitting small connected components. Column (c) shows the SVM

skin detection results where the utilized training samples are the same as those which were used to create the QPC. It is evident that in equal condition (using the same sample images), these results are not accurate at all. For a proper classification, SVM should be particularly trained with the training samples extracted from the test image. Finally, column (d) shows the best possible results when the SVM is trained with sub-images extracted from the test image. Here, the samples have chosen from different part of skin and non-skin regions to increase the accuracy of SVM results. The size of training samples is 30×30 pixels, same as those employed in our method. Comparing the misclassifications in columns (b) and (d), it is observed that even the SVM in its best performance has more false positives than the proposed method.

Table 1. Time Performance of the Proposed Skin Detection Method on Different Sized Images.

Image Size (pixels)	588×334	896×592	512×715	380×253
Elapsed Time (seconds)	1.722	3.372	2.494	1.216

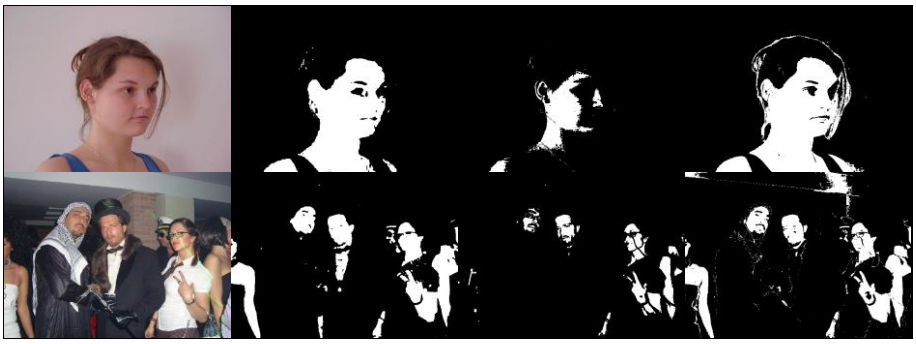

(a) (b) (c) (d)

Fig. 8. Comparison of the proposed method with the SVM. a) The original image. b) detection results with the proposed method. c) SVM detection results when the training samples are the same as QPC. d) SVM detection results when the samples are exclusively extracted from the image.

Although, the proposed skin detection method is not pixel-based, and does not process the color information of each single pixel, but the results accuracy are comparable with pixel-based methods. As a benchmark, our method is compared with one well-known pixel based skin detection methods presented in [42] in Fig. 9.

Finally, we have shown some images in which the misclassification of the proposed method is considerable due to the color properties of the non-skin/background. Since color features in their simplest way have been utilized, it is obvious that a linear classifier like ours can make inevitable mistakes. Fig. 10 shows some of these images that the elimination of small connected components cannot refine the results.

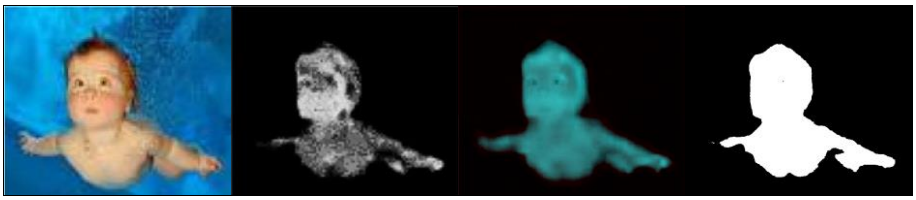

(a) (b) (c) (d)

Fig. 9. Comparison of the proposed method with one of the pixel-based skin detection methods. a) The original image. b) The obtained results by [42]. c) The obtained results in the QPC. d) The final skin detection results of our method.

(a) (b) (c)

Fig. 10. Some of the images that contain large areas as false positives before the final stag e of eliminating small connected components. a) The original images. b) The images converted to the QPC. c) Detection results after applying Otsu's method.

4. Conclusion and Future Work

A new color space was introduced which has the ability to discriminate skin regions using some sample color features. The conversion to the new space (QPC) uses a 3×3 conversion matrix through a linear conversion equation. The matrix was obtained by solving the quadratic cost function of the distances between skin and non-skin pixel samples. The proposed method can be used in skin classification in a variety of images without being trained. The well-known Otsu's thresholding method was applied on the achieved image in the QPC to binarize the image, and show skin and non-skin regions in white and black respectively. The innovation of the presented method is utilizing quadratic programming, a renowned optimization technique of advanced mathematics, in pattern recognition. In addition, the method is very simple since it utilizes color features from the RGB color space directly, and fast since it is applicable with a simple matrixes multiplication followed by an elimination of small falsely detected regions. The QPC can also effectively be applied for target detection in other applications such as skin disease detection. Adding more features in form of texture, spatial or color from other color spaces could also improve the discrimination abilities of the QPC.

References

[1] Gonzalez, R. C., & Woods, R. E. (2008). *Digital Image Processing* (3rd ed.). New York: Pearson Education/Prentice Hall, Upper Saddle River.

[2] Yang, M. H., & Ahuja, N. (1998). Detecting human faces in color images. *Proceedings of the International Conference on Image Processing (ICIP), Vol. 1* (pp. 127–139).

[3] Gabrys, B., & Bargiela, A. (2000). General fuzzy min-max neural network for clustering and classification. *IEEE Trans Neural Network, 11(3)*, 769–783.

[4] Tao, L. M., Peng, Z. Y., & Xu, G. Y. (2001). Features of skin color. *J Softw, 12(7)*, 1032–1041.

[5] De Dios, J. J., & Garcia, N. (2003). Face detection based on a new color space YCgCr. *Proceedings of International Conference on Image Processing (ICIP), Vol. 3* (pp III-909-12).

[6] Zhao, Y. J., Dai, S. L., & Xi, X. (2008). A Mumford-Shah level-set approach for skin segmentation using a new color space. *Proceedings of 7th International Conf. on Sys. Simulation and Scientific Computing (ICSC)* (pp 307–310).

[7] Stehle, T., Behrens, A., & Aach, T. (2008). Enhancement of visual contrast in fluorescence endoscopy. *Proceedings of IEEE International Conference on Multimedia and Expo (ICME)* (pp 537–540).

[8] Jia, L., & Liu, Y. (2008). A novel thresholding approach to background subtraction. *IEEE Workshop on Applications of Computer Vision (WACV), Copper Mountain, CO,* 1–6.

[9] Park, J. B. (2004) Detection of specular highlights in color images using a new color space transformation. *Proceedings of IEEE International Conference on Robotics and Biomimetics (ROBIO)* (pp 737–741).

[10] Panetta, K., Qazi, S., & Agaian, S. (2008). Techniques for detection and classification of edges in color images. *Proceedings of (SPIE), Vol. 6982* (pp. 69820W–69820W-11).

[11] Mirghasemi, S., Yazdi, H. S., & Lotfizad, M. (2011). A target-based color space for sea target detection. *Applied Intelligence, Springer.*

[12] Erzhong, H., Hidenori, S., Hirokazu, N., Eiichi, T., Yasuo, S., Ken, T., Hiroshi, A., & Masahiro, M. (2016). Bleeding and tumor detection for capsule endoscopy images using improved geometric feature. *Journal of Medical and Biological Engineering, 36 (2016),* 344-56.

[13] Amin, K., Saeed, M., Abbas, K., Chee Peng, L., & Saeid, N. (2017). A new PSO-based approach to fire flame detection using k-medoids clustering. *Expert Systems with Applications, 68,* 69-80.

[14] Zhang, L., & Zhang, Y. (2017). Airport detection and aircraft recognition based on two-layer saliency model in high spatial resolution remote-sensing images. *IEEE Journal of Selected Topics in Applied Earth Observations and Remote Sensing*, *10(4),* 1511-1524.

[15] Marcos Eduardo, V., & Raul Ambrozio, V. (2017). Mathematical morphology on the spherical cielab quantale with an application in color image boundary detection. *Journal of Mathematical Imaging and Vision, 57 (2017),* 183-201.

[16] Zhang, Y. Y., Qin, Y., Lv, X. D., & Zhang, P. (2016). Saliency detection via Pca of image patches and Ica-R. *Multimedia Tools and Applications, 75 (2016),* 4527-42.

[17] Wang, X. Y., Wang, T., & Bu, J. (2011). Color image segmentation using pixel wise support vector machine classification. *Pattern Recognition, 44(4)*, 777–787.

[18] Wang, X. Y., Wang, Q. Y., Yang, H. Y., & Bu, J. (2011). Color image segmentation using automatic pixel classification with support vector machine. *Neurocomputing, 74(18)*, 3898–3911.

[19] Mathanker, S. K., Weckler, P. R., Bowser, T. J., Wang, N., & Maness, N. O. (2011). Ada Boost classifiers for pecan defect classification. *Computers and Electronics in Agriculture, 77(1)*, 60–68.

[20] Wang, X. Y., Zhang, X. J., Yang, H. Y., & Bu, J. (2012). A pixel-based color image segmentation using support vector machine and fuzzy *C*-means. *Neural Networks, 33,* 148–159.

[21] Rivera, M.; Dalmau, O., & Tago, J. Image segmentation by convex quadratic programming. *Proceedings of 19th International Conference on Pattern Recognition, ICPR 2008* (pp. 1-5).

[22] Fu, Z., & Robles-Kelly, A. A quadratic programming approach to image labelling. *IET Computer Vision, 2(4),* 193-207.

[23] Brand, M., & Chen, D. H. (2011). Parallel quadratic programming for image processing. *Proceedings of 18th IEEE International Conference on Image Processing (ICIP)* (pp. 2261–2264).

[24] Rivera, M., & Dalmau, O. (2012). Variational viewpoint of the quadratic Markov measure field models: Theory and algorithms. *IEEE Transactions on Image Processing, 21(3)*, 1246-1257.

[25] Pavan, M., & Pelillo, M. (2003). Image segmentation by dominant sets. *Electronic Notes in Discrete Mathematics, 9th International Workshop on Combinatorial Image Analysis, 12*, 166–177.

[26] Toshev, A., Taskar, B., & Daniilidis, K. (2010). Object detection via boundary structure segmentation. *Proceedings of IEEE Conference on Computer Vision and Pattern Recognition (CVPR)* (pp. 950 – 957).

[27] Yang, Y., & Li, S. P. (2011). A maximum margin segmentation selection for visual object detection. *Proceedings of International Conference on Intelligent Computation Technology and Automation (ICICTA)*, *Vol. 2*, (pp. 344 – 349).

[28] Zacharaki, E. I., & Bezerianos, A. Abnormality segmentation in brain images via distributed estimation. *IEEE Transactions on Information Technology in Biomedicine, 16(3),* 330 - 338.

[29] Lempitsky, V. (2010). Surface extraction from binary volumes with higher-order smoothness. *Proceedings of IEEE Conference on Computer Vision and Pattern Recognition (CVPR),* (pp. 1197–1204).

[30] Abdel-Malek, L. L., & Areeractch, N. (2007). A quadratic programming approach to the multi-product newsvendor problem with side constraints. *Eur J Oper Res*, 176, 855–61.

[31] Ammar, E., & Khalifa, H. A. (2003). Fuzzy portfolio optimization: a quadratic programming approach. *Chaos, Solitons & Fractals*, *18,* 1045–54.

[32] Dwyer, T., Koren, Y., & Marriott, K. (2006). Drawing directed graphs using quadratic programming. *IEEE Trans Vis Comput Gr, 12*, 536–48.

[33] Pavlovic´, L., & Divnic´, T. (2007). A quadratic programming approach to the Randic´ index. *Eur J Oper Res, 176*, 435–44.

[34] Petersen, J. A. M., & Bodson, M. (2006). Constrained quadratic programming techniques for control allocation. *IEEE Trans Control Syst Technol, 14*, 91–8.

[35] Schwarz, H. G. (2006). Economic material-product chain models: Current status, further development and an illustrative example. *Ecol Econ*, *58*, 373–92.

[36] Zhang, W. G., & Nie, Z. K. (2005). On admissible efficient portfolio selection policy. *Appl Math Comput, 169*, 608–23.

[37] Weszka, J. S., Nagel, R. N., & Rosenfeld, A. (1974). A threshold selection technique. *IEEE Trans. Comput., C-23,* 1322 -1326.

[38] Watanabe, S., & CYBEST Group. (1974). An automated apparatus for cancer prescreening: CYBEST. *Comp. Graph. Imiage Process, 3*, 350—358.

[39] Chow, C. K., & Kaneko, T. (1972). Automatic boundary detection of the left ventricle from cineangiograms. *Comput. Biomed. Res., 5*, 388-410.

[40] Otsu, N. (1979). A threshold selection method from gray-level histograms. *IEEE Transactions on Systems, Man, and Cybernetics, 9(1),* 62-66.

[41] Haralick, R. M., & Shapiro, L. G. (1992). *Computer and Robot Vision, I, Addison-Wesley,* 28-48.

[42] Sanaa El, F., Mohamed, D., & Driss, A. (2008). The mixture of K-optimal-spanning-Trees based probability approximation: Application to skin detection. *Image and Vision Computing, 26,* 1574–1590.

Ali Khayati received the B.S degree in computer engineering (hardware design) from University of Tehran, Iran in 1998 and M.S in computer architecture from Iran University of Science and Technology, Iran in 2001. He is currently a Ph.D candidate at IUST and faculty member at IAU, Parand branch. His research interests are digital design, ASIC design, and image processing.

Saeed Mirghasemi received his BE and ME in electrical engineering in 2006, and 2009 respectively. He started at Victoria University of Wellington (VUW) as a Ph.D student in computer science (2013), then a postdoctoral fellow (2017), and now a teaching fellow at School of Engineering and Computer Science. His area of research is image processing, evolutionary computation, and data mining.